UC Merced

UC Merced Previously Published Works

Title

Comparative genomics of two ‘Candidatus Accumulibacter’ clades performing biological phosphorus removal

Permalink

https://escholarship.org/uc/item/97h283wn

Journal

The ISME Journal: Multidisciplinary Journal of Microbial Ecology, 7(12)

ISSN

1751-7362

Authors

Flowers, Jason J

He, Shaomei

Malfatti, Stephanie

et al.

Publication Date

2013-12-01

DOI

10.1038/ismej.2013.117

Peer reviewed

eScholarship.org Powered by the California Digital Library
University of California

The ISME Journal (2013) 7, 2301–2314
© 2013 International Society for Microbial Ecology All rights reserved 1751-7362/13
www.nature.com/ismej

ORIGINAL ARTICLE

Comparative genomics of two '*Candidatus* Accumulibacter' clades performing biological phosphorus removal

Jason J Flowers[1], Shaomei He[2], Stephanie Malfatti[2], Tijana Glavina del Rio[2], Susannah G Tringe[2], Philip Hugenholtz[3] and Katherine D McMahon[1]
[1]*Departments of Civil and Environmental Engineering, and Bacteriology, University of Wisconsin at Madison, Madison, WI, USA;* [2]*US Department of Energy Joint Genome Institute, Walnut Creek, CA, USA and* [3]*Australian Centre for Ecogenomics, University of Queensland, St Lucia, Queensland, Australia*

Members of the genus *Candidatus* Accumulibacter are important in many wastewater treatment systems performing enhanced biological phosphorus removal (EBPR). The Accumulibacter lineage can be subdivided phylogenetically into multiple clades, and previous work showed that these clades are ecologically distinct. The complete genome of *Candidatus* Accumulibacter phosphatis strain UW-1, a member of Clade IIA, was previously sequenced. Here, we report a draft genome sequence of *Candidatus* Accumulibacter spp. strain UW-2, a member of Clade IA, assembled following shotgun metagenomic sequencing of laboratory-scale bioreactor sludge. We estimate the genome to be 80–90% complete. Although the two clades share 16S rRNA sequence identity of >98.0%, we observed a remarkable lack of synteny between the two genomes. We identified 2317 genes shared between the two genomes, with an average nucleotide identity (ANI) of 78.3%, and accounting for 49% of genes in the UW-1 genome. Unlike UW-1, the UW-2 genome seemed to lack genes for nitrogen fixation and carbon fixation. Despite these differences, metabolic genes essential for denitrification and EBPR, including carbon storage polymer and polyphosphate metabolism, were conserved in both genomes. The ANI from genes associated with EBPR was statistically higher than that from genes not associated with EBPR, indicating a high selective pressure in EBPR systems. Further, we identified genomic islands of foreign origins including a near-complete lysogenic phage in the Clade IA genome. Interestingly, Clade IA appeared to be more phage susceptible based on it containing only a single Clustered Regularly Interspaced Short Palindromic Repeats locus as compared with the two found in Clade IIA. Overall, the comparative analysis provided a genetic basis to understand physiological differences and ecological niches of Accumulibacter populations, and highlights the importance of diversity in maintaining system functional resilience.
The ISME Journal (2013) **7,** 2301–2314; doi:10.1038/ismej.2013.117; published online 25 July 2013
Subject Category: Integrated genomics and post-genomics approaches in microbial ecology
Keywords: enhanced biological phosphorus removal; '*Candidatus* Accumulibacter phosphatis'; activated sludge

Introduction

Enhanced biological phosphorus removal (EBPR) is an activated sludge process used worldwide to remove phosphorus from wastewaters. Bacteria conducting EBPR do so by accumulating large quantities of polyphosphate inside their cells, presumably in response to alternating anaerobic and aerobic conditions in the activated sludge tank (Mino *et al.*, 1998). An archetypal EBPR organism is readily enriched with acetate as a primary carbon source in laboratory-scale sequencing batch reactors (Oehmen *et al.*, 2007; McMahon *et al.*, 2010), and is named '*Candidatus* Accumulibacter phosphatis' (Hesselmann *et al.*, 1999) (henceforth referred to as Accumulibacter). The Accumulibacter lineage is phylogenetically subdivided into two types (Types I and II) based on comparative sequence analysis of the gene encoding polyphosphate kinase (*ppk1*) (McMahon *et al.*, 2002). Each type is comprised of several coherent clades exhibiting unique distribution patterns in wastewater treatment systems (He *et al.*, 2007; He *et al.*, 2010a) and natural aquatic environments (Peterson *et al.*, 2008).

Correspondence: KD McMahon, Departments of Civil and Environmental Engineering, and Bacteriology, University of Wisconsin at Madison, 1550 Linden Drive, 5525 Microbial Science Building, Madison, WI 53706, USA.
E-mail: tmcmahon@engr.wisc.edu
Received 6 December 2012; revised 14 May 2013; accepted 11 June 2013; published online 25 July 2013

Comparative genome analysis can reveal factors that identify genes or pathways that relate to niche dimensions. Differential gene content can at least partly explain the segregation of *Prochlorococcus* ecotypes between high- and low-light conditions in the ocean (Kettler *et al.*, 2007). A recent paper that compared the genomes of *Salinispora* species discovered several genes required for marine life adaption (Penn and Jensen, 2012). Comparisons among strains or populations within a species often point to evolutionary-scale forces shaping genomes, such as selection and recombination. A comparison of seven isolated *Sulfolobus islandicas* strains isolated from three geographically sites revealed extensive gene loss and gain from recombination within these populations using mobile elements to maintain genetic diversity (Reno *et al.*, 2009). More recently, metagenomics has enabled such comparisons among uncultured organisms (Gilbert and Dupont, 2011). Accumulibacter-enriched sludge was the subject of a metagenomic sequence analysis (Garcia Martin *et al.*, 2006) that eventually resulted in the completion of the genome for Accumulibacter Clade IIA strain UW-1 (GenBank CP001715, Goldstamp Gc01096, hereafter referred to as 'Clade IIA UW-1'). The resulting genome consisted of a 5.1-Mbp chromosome and three plasmids. The genome sequencing clarified several features of EBPR metabolism that had been contentious (Garcia Martin *et al.*, 2006; Oehmen *et al.*, 2007). Most notably, it confirmed that the Embden–Meyerhof–Parnas pathway for glycolysis was fully present and also revealed that Accumulibacter had genes for nitrogen and carbon fixation. The latter was unexpected considering the carbon- and nitrogen-rich characteristics of wastewater. In addition, a novel cytochrome that consisted of a fusion of cytochrome *b*/*b*6, several transmembrane domains and a nicotinamide adenine dinucleotide/flavin adenine dinucleotide (NAD/FAD)-binding site was identified and proposed to allow for anaerobic tricarboxylic acid cycle (TCA cycle) operation.

Recent work has revealed ecophysiological differences among Accumulibacter clades. Two morphologically distinct Accumulibacter populations were enriched using different carbon sources and found to have different nitrate reduction abilities (Carvalho *et al.*, 2007). Subsequently, Flowers *et al.* (2009) observed that Clade IA-enriched sludge could couple phosphorus uptake with nitrate reduction, whereas Clade IIA could not. Wexler *et al.* (2009) investigated the protein expression of two EBPR bioreactors enriched with different Accumulibacter clade composition using radio-labeled proteomics. One bioreactor revealed enhanced TCA cycle gene expression aerobically, whereas the other showed enhanced synthesis anaerobically, suggesting that these two Accumulibacter populations had distinct anaerobic and aerobic metabolisms. Another study explored the impact of polyphosphate content on anaerobic performance and stoichiometry, and found that when polyphosphate content decreased in the cells, Clade IIA appeared to switch to a glycogen-accumulating metabolism, which no longer assisted in removing phosphate from the system (Acevedo *et al.*, 2012). These findings suggest that distinct Accumulibacter clades inhabit different niches in EBPR ecosystems, each providing an important role in ecosystem function.

Several recent studies have assessed Accumulibacter gene expression using metaproteomics, metatranscriptomics or reverse transcription quantitative real-time polymerase chain reaction (qPCR) (Burow *et al.*, 2008; Wilmes *et al.*, 2008; Wexler *et al.*, 2009; He *et al.*, 2010b; He and McMahon, 2011). However, such analyses have proven difficult because multiple strains of Accumulibacter usually coexist in activated sludges, whereas only the Clade IIA UW-1 genome is available as a reference. Therefore, we sequenced the metagenome of a Clade IA-enriched community to generate a Clade IA reference genome and to better understand ecophysiological and genomic differences between Accumulibacter clades. By developing a greater understanding of the genomic basis underlying hypothesized distinct niches for the clades, we will also be able to provide more accurate models that help to predict the overall performance of EBPR systems (Oehmen *et al.*, 2010c).

Materials and methods

Sample collection and processing

The operation of the lab-scale acetate-fed sequencing batch reactor was described as the 'US sludge' in Garcia Martin *et al.* (2006), except that the pH was controlled at 7.0–7.5, and $4\,mg\,l^{-1}$ of allylthiourea was added to the reactor to inhibit nitrification (for more details see Supplementary Online Material).

A biomass sample was collected from the sequencing batch reactor on 21 December 2007 for metagenomic sequencing. Community genomic DNA was extracted from ~0.2-g cell pellet using an enzymatic digestion method described previously (Garcia Martin *et al.*, 2006). At the same time, fluorescence *in situ* hybridization using the PAOMIX probes (Crocetti *et al.*, 2000) was performed as described previously (He *et al.*, 2008) to estimate the total Accumulibacter abundance. Also, *ppk1*-targeted qPCRs were conducted, as described previously (He *et al.*, 2007), to determine relative proportions of the two Accumulibacter clades.

Metagenomic sequencing

The extracted genomic DNA was used for sequencing with three different technologies: (1) two whole genome shotgun libraries with 3- (plasmid) and 40-kb (fosmid) inserts in pUC18 and pCC1FOS, respectively, were end-sequenced with the Sanger

technology as described previously (Garcia Martin *et al.*, 2006); (2) two runs of pyrosequencing with the Roche 454 GS-FLX system and Titanium chemistry, including one using a 15-kbp paired-end library; and (3) one lane of paired-end (2×76 bp) Illumina GA II (San Diego, CA, USA).

Metagenome assembly

To avoid a mosaic assembly between Clades IA and IIA, sequences generated from the paired-end Illumina run were screened to remove reads that shared high sequence identities (i.e. $\geqslant 97\%$) to Clade IIA UW-1 using the runMapping module of Newbler version 2.4 (454 Life Sciences, Branford, CT, USA). Following screening, raw reads were assembled using Velvet assembler (v.1.0.10) (Zerbino and Birney, 2008) with a hash length of 57, a minimum contig length of 200 bp and a paired-end insert size of 300 bp. The hash length of 57 was chosen over lengths of 4151, and 61 based on contig N50, total contig size, total number of contigs and maximum contig size. The Velvet-assembled contigs were then shredded into 1800-bp fragments that overlapped by 900 bp. For 454 reads, dinucleotide repeats were removed using Newbler, and redundant reads were removed by Cd-hit versions 2007-0131 (Li and Godzik, 2006) with a requirement of 100% sequence identity on the initial 10 bp and 90% identity on the entire read. Both 454 and Sanger reads were trimmed to an accuracy of 97% using Lucy v.1.19p (Chou and Holmes, 2001), followed by a screen using the runMapping module of Newbler v.2.4 to remove reads that were $\geqslant 97\%$ identical to Clade IIA UW-1. The final set of 454 reads, Sanger reads and fragmented Velvet contigs were assembled using Newbler v.2.4 with a minimum identity of 98% and a minimum word length of 80 bp.

Accumulibacter Clade IA scaffold binning and annotation

To identify scaffolds derived from Accumulibacter Clade IA, tetranucleotide frequency analysis was performed (Teeling *et al.*, 2004). Briefly, the frequencies of all 256 possible tetranucleotides were determined for each DNA scaffold using a custom Perl script. Because the scaffolds were assembled from contigs based on paired-end reads, large regions within scaffolds contained no sequence data. To ensure that the scaffolds were not constructed from contigs from multiple organisms, the scaffolds were broken into pieces where Ns were present and analyzed as separate fragments. In addition, these fragments were screened to remove those that were smaller than 20 kbp. In a previous study using self-organizing maps, it was found that 10-kbp fragments were required for accurate phylogenetic binning (Abe *et al.*, 2003); therefore, 20 kbp was chosen to improve accuracy. To provide a reference for phylogenetic binning, 11 complete genomes from organisms related to those detected in previous 16S rRNA gene clone libraries, as well as the Accumulibacter Clade IIA UW-1 genome, were shredded into 50-kb fragments and analyzed for tetranucleotide frequency separately. The resulting 66 unknown fragments from the metagenome and the 3086 fragments from representative organisms were then analyzed and plotted using correspondence analysis in the R software package (R Development Core Team, 2009). Based on the ordination patterns from correspondence analysis, fragments clustered with Accumulibacter Clade IIA UW-1, but distinct from other organisms, were considered putative Clade IA fragments. For fragmented scaffolds, at least half of the fragments had to be classified as Clade IA for the scaffold to be considered as being derived from Clade IA. A total of seven putative Accumulibacter Clade IA scaffolds were identified and annotated using the RAST server (Aziz *et al.*, 2008). The resulting annotation had 3877 protein coding sequences and 42 tRNA genes.

Ortholog identification

Genes from Clade IA were compared with the genes of Clade IIA UW-1 and *vice versa*, using blastn (Altschul *et al.*, 1997), to identify orthologs between the two genomes with the following blast parameters modified from Rusch *et al.* (2007) to detect sequences with up to 45% divergence: blastall $-$p blastn $-$F 'm l' $-$m 8 $-$r 8 $-$q $-$8 $-$X 150 $-$e 1e$-$5. The blast results were then screened to remove any alignment that was $<40\%$ of the gene length. From the resulting blast output, putative orthologs were identified by examining reciprocal (or bi-directional) best blast hits.

Calculation of synonymous and non-synonymous substitution ratio

Each pair of amino-acid sequences for all orthologs identified during reciprocal best blast-hit analysis was aligned using MUSCLE (v.3.8.31 default parameters) (Edgar, 2004). The resulting alignments and the nucleotide sequences for each pair were then used to create a codon-based alignment using PAL2NAL (v.14 default parameters) (Suyama *et al.*, 2006). The resulting codon-based DNA alignment for each pair was then analyzed using the codeml package from PAML (v.4) (Yang, 2007) to estimate the synonymous and non-synonymous substitution ratio based on maximum likelihood.

Analysis of genome synteny

To evaluate the differences in genomic structure between Clade IIA UW-1 genome and the Clade IA scaffolds, these sequences were aligned using the Artemis Comparison Tool (Carver *et al* 2005). The default parameters were used for the megablast

alignment as the input for Artemis Comparison Tool including a maximum expected value of 1e − 4. To increase our ability to detect syntenic regions, adjacent syntenic regions that were <1 kbp apart (~1 gene) were joined to allow for a single gene insertion. The total length of syntenic regions was determined by summing the lengths of all of these regions, which were at least 2 kbp long.

Genomic islands

Clade IA genomic islands (GIs) were identified by blasting all genes from Clade IIA UW-1 genome against the Clade IA scaffolds with the following parameters: blastall −p blastn −m 8 −e 1e − 4 −r 8 −q −8 −X 150 −F 'm l'. Blast results were then screened to remove any alignment that was <40% of the gene length, and for each gene the blast result with the highest bit score was selected. Once the blast results were mapped onto the Clade IA scaffolds, GIs were identified as regions at least 20 kbp in length without any blast alignments. The process was repeated to find Clade IIA UW-1 GIs by blasting all genes from Clade IA scaffolds against the Clade IIA UW-1 genome. For each identified GI, the Codon Usage Deviation, defined as the sum of difference of codon use for each triplet between each island and the scaffolds/genome, was determined using the European Molecular Biology Open Software Suite (EMBOSS) package CUSP and CODCMP (Rice *et al.*, 2000).

Results

Sequencing, assembly and binning of Clade IA scaffolds

A biomass sample was collected from a laboratory-scale bioreactor that was continuously maintaining the same activated sludge biomass that was previously sampled for metagenomic sequencing in 2004 (Garcia Martin *et al.*, 2006). However, in contrast to the 2004 sample, the community was enriched in Clade IA rather than Clade IIA (Table 1). We will use the nomenclature in Table 1 to discuss the two samples hereafter.

Sample R107-IA was subjected to metagenomic sequencing using a combination of technologies: traditional Sanger 3-kb plasmid end sequencing (109 Mbp), Sanger 40-kbp fosmid end sequencing (8 Mbp), 454 Titanium Shotgun (238 Mbp), 454 Titanium Paired End (178 Mbp) and Illumina Paired End (2392 Mbp) (Supplementary Table S1). This effort generated a total of 2827 Mbp of sequence. Before assembly, we removed reads sharing ⩾97% nucleotide identity with the finished Clade IIA UW-1 genome to prevent false mosaic assemblies of Clade IIA reads into Clade IA contigs, as Clade IIA was still present in the community (Table 1). After this preassembly screen, 95% of the reads remained (Supplementary Table S1), and were assembled into 18 776 contigs (25.1 Mbp), with a largest contig of length 85 kbp. The contigs were then joined into 1466 scaffolds (173 Mbp), with a largest scaffold of length 2.75 Mbp (Figure 1).

We used tetranucleotide frequency analysis to identify scaffolds that were putatively derived from Accumulibacter Clade IA (Figure 2). A large number of the R107-IA scaffold fragments clustered with the Clade IIA UW-1 fragments, and were distinct from fragments from other reference genomes. Based on these results, a total of seven putative Accumulibacter Clade IA scaffolds were identified, amounting to 4.5 Mbp of sequence (4.2 Mbp when excluding Ns) with an average GC content of 64%. These seven Clade IA scaffolds (Supplementary Table S2) were annotated using the RAST server, yielding 3923 predicted genes (Table 2). In comparison, the Accumulibacter Clade IIA UW-1 chromosome and three plasmids totaled 5.3 Mbp of sequence and had 4792 predicted genes. We also identified a *ppk1* homolog in the largest scaffold (Scaffold01135) sharing 98% nucleotide identity with a Clade IA

Table 1 Community composition in the two metagenomic samples

	Samples	
	R104-IIA	*R107-IA*
Collection date	30 June 2004	21 December 2007
% Accumulibacter[a]	~80%	~40%
% Clade IA[b]	7%	89%
% Clade IIA[c]	93%	11%

Abbreviation: ANI, average nucleotide identity; DAPI, 4',6-diamidino-2-phenylindole; FISH, fluorescene *in situ* hybridization; qPCR, quantitative real-time polymerase chain reaction.
[a]Approximate fraction of total DAPI-stained cells that were hybridized by FISH with PAOMIX probes.
[b]Fraction of total Accumulibacter *ppk1* genes that were affiliated with Clade IA based on qPCR.
[c]Fraction of total Accumulibacter *ppk1* genes that were affiliated with Clade IIA based on qPCR.

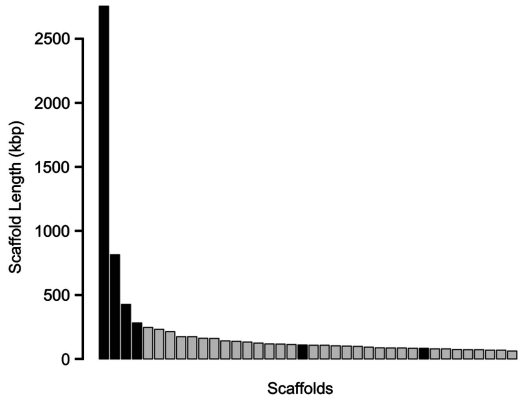


Figure 1 Scaffold lengths of the 40 longest scaffolds from the R107-IA metagenome. Bars shown in black represent scaffolds that were identified as Clade IA scaffolds based on tetranucleotide frequencies.

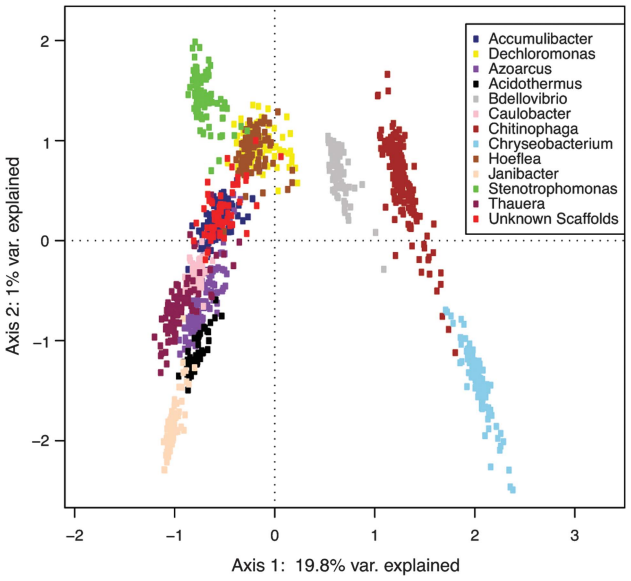


Figure 2 Correspondence analysis of metagenomic fragments and representative genomic fragments of taxa found in sample R107-IA using tetranucleotide frequencies patterns. Each point represents either a metagenomic scaffold fragment or a genomic fragment. Genomic fragments are identified using color coding shown in the legend.

Table 2 Genome features

	Clade IIA UW-1 genome		*Clade IA UW-2 scaffolds*
Number of bases (Mbp)	5.3		4.5
GC content (%)	64		64
Total ORFs	4792		3923
Function assigned	3127		2704
Hypothetical proteins	1665		1219
Shared genes		2317	
Exclusive genes	2475		1606
rRNA operons	2		ND[a]
tRNAs	49		42
ANI (%)		78.3	
Average ORF size (bp)	1012		924

Abbreviations: ANI, average nucleotide identity; GC, guanine–cytosine; ND, not determined; ORF, open reading frame.
[a]rRNA operons were not determined since rRNA reads were likely removed during the preassembly screen because of the high sequence identity of rRNA genes between Clades IA and IIA.

ppk1 identified previously (GenBank AF502200.1; McMahon *et al.*, 2002). As this locus was originally used to define the Accumulibacter clade phylogeny, the presence of a Clade IA *ppk1* homolog within this putative Clade IA scaffold provides confidence that the scaffolds were assembled and binned properly.

We examined the seven putative Clade IA scaffolds to determine genome completeness. Forty-two of the 49 tRNAs annotated in the finished Clade IIA UW-1 genome were identified by blastn. All of the 52 ribosomal proteins and 16 of 20 tRNA synthetases were identified by tblast. We also conducted a Cluster of Orthologous Genes (COG)-based analysis by first determining all of the COG functions shared among the four neighboring Rhodocyclaceae sequenced genomes besides Clade IIA UW-1 (*Aromatoleum aromaticum* EbN1, *Dechloromonas aromatica* RCB, *Azoarcus* sp. BH72 and *Thauera* sp. MZ1T), yielding 1273 COG functions that were at least present once in all of the four neighbors. This COG list was then compared with a similar list for the Accumulibacter Clade IA scaffolds, and it was determined that 119 (~10%) of the COG functions were missing from Clade IA scaffolds. The average copy number of each COG function was then determined for these four neighbor genomes, and the average abundance was compared with Clade IA scaffolds. From this method, it was determined that Clade IA lacked roughly 20% of the COG functions. Therefore, the genome was estimated to be roughly 80–90% complete.

Genome alignment analysis

To visualize the structural differences between the two genomes, the Accumulibacter Clade IA scaffolds were aligned against the Clade IIA UW-1 chromosome and three plasmids (Supplementary Figure S1). The order of the Clade IA scaffolds was determined by using the contig reordering function in Mauve v.2.3.1 (Darling *et al.*, 2010) using the Clade IIA UW-1 genome as a reference. The alignments clearly show that the two genomes have significantly different structure. Considering that the two strains share 98.7% identity in their 16S rRNA genes, the amount of difference in genome structure is surprising.

The largest syntenous region between the two genomes was 10.5 kbp long; however, only 206 regions were >2000 bp (~2 genes long), which totaled 623 kbp. If syntenous regions that were <1000 bp apart (~<1 gene) were merged and any region <2000 bp when combined was removed, a total of 236 syntenic regions that total just under 1 Mbp in length remained. This accounts for ~25% of the Clade IA genome. It is possible that this number is underestimated because of the removal of potentially highly conserved regions during the preassembly sequence screening that removed sequences <97% similar to Clade IIA, which likely resulted in gaps in the Clade IA scaffolds. Therefore, the Clade IA genome should be completed to verify these results.

Shared and differential gene content

We compared the genes shared between the two clades using Reciprocal Best Hit Analysis. A total of 2317 genes and 2410 proteins were identified as shared between the two clades based on nucleotide and protein sequence, respectively (Table 2), although this is a conservative estimate because the Clade IA genome is not finished. These genes share an average nucleotide identity (ANI) of 78.3% (Figure 3) and constitute 49% of the total Clade IIA UW-1 genes.

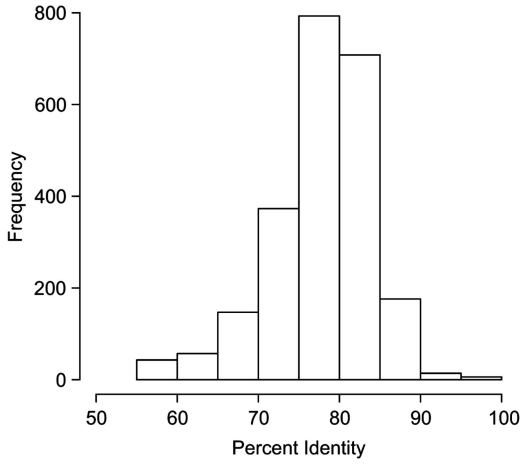


Figure 3 Histogram of ANI (ANI) shared between Clade IIA UW-1 genes and putative Clade IA genes. ANI was calculated for reciprocal best BLASTN hits.

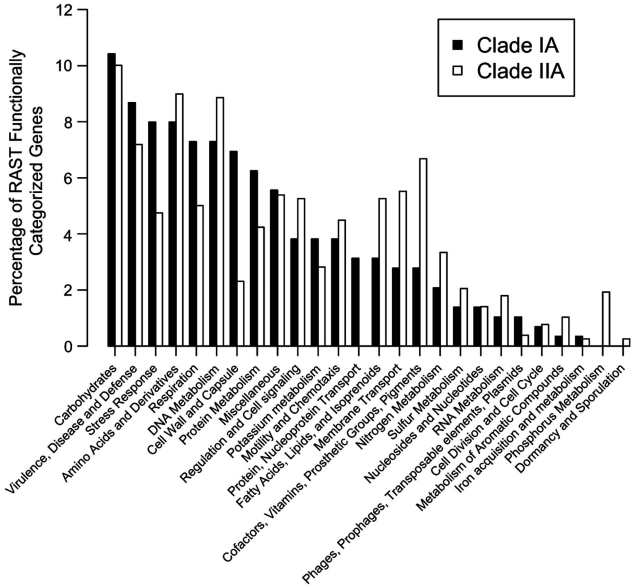


Figure 4 Distribution of RAST Functional Categories of 'unique' (non-orthologous) genes in Accumulibacter Clades IA and IIA expressed as a percentage of each category relative to the total number of unique RAST functionally categorized genes in each genome.

Surprisingly, scaffolds from Clade IA matched to genes on the plasmids from Clade IIA UW-1. Specifically, Scaffold00037 contained both conjugation genes to allow for genetic exchange between two bacteria from one of the plasmids as well as genes from the Clade IIA UW-1 chromosome including genes for development of precursors for Vitamin B12 synthesis, which is an important cofactor in many metabolic reactions. Also, Scaffold01134 contained genes from all three Clade IIA UW-1 plasmids as well as a few from the Clade IIA UW-1 chromosome. In contrast, Scaffold000028, which is the smallest Clade IA scaffold (35 kbp), only had a single Reciprocal Best Hit Analysis with Clade IIA UW-1. Although the majority of the genes (~80%) on Scaffold000028 were hypothetical, a few genes were phage-related, which suggests that these genes may be remnants of a lysogenic phage (discussed below) that carried these genes into the genome.

Genes from both clades were functionally classified according to RAST Functional Categories (Aziz *et al.*, 2008) and the frequency of each category was compared in both genomes (Supplementary Figure S2). We found minimal differences in RAST Functional Category distribution, despite the fact that ~50% of the genes are non-orthologous based on the Clade IIA UW-1 gene count. To understand some of the functional differences between Clade IA and IIA, the distribution of RAST Functional Category for genes unique (non-orthologous) to both clades was analyzed (Figure 4). Most categories were comparably represented within the two genomes, but several categories appeared to be enriched in Clade IA, including 'Stress Response', 'Respiration', 'Cell Wall and Capsule' and 'Protein, Nucleoprotein transport'. Several categories were enriched in Clade IIA UW-1, including 'Fatty Acid, Lipids, and Isoprenoids', 'Membrane Transport', 'Cofactors, Vitamins, Prosthetic Groups, Pigments' and 'Phosphorus Metabolism.' Considering these latter categories are related to basic cell physiology, it is possible that these highly conserved sequences were removed during the preassembly screen and not incorporated into the final Clade IA genome.

Genomic islands

We used the finished Clade IIA UW-1 genome to recruit genes from the Clade IA scaffolds to identify relatively large regions of the Clade IIA UW-1 genome that may be absent in the Clade IA genome (GIs). Twenty-eight putative Clade IIA UW-1 GIs were identified that contained 575 genes (Table 3). The largest GI was 41 kbp. Of these genes, 270 (~46%) were hypothetical proteins. Of the 28 GIs, 16 contained some elements of foreign DNA based on the presence of phage, transposase or integrase genes, which likely explains why these regions contained unique genes. Another GI contained several genes affiliated with Clustered Regularly Interspaced Short Palindromic Repeats (CRISPRs), which have been linked to phage immunity (Barrangou *et al.*, 2007) (also discussed later). Surprisingly, GI 21, which had the largest codon usage deviation, did not contain any evidence of a foreign DNA source, such as phage, transposase or integrase genes. Despite having apparent remnants of foreign DNA, the 16 GIs with phage, transposase or integrase genes had comparable codon usage deviation to GIs without these genes. This suggests that the genes within these 16 GIs were either present in an ancestral lineage from which both clades were derived and subsequently lost in Clade

Table 3 Characteristics of Accumulibacter Clade IIA UW-1 GIs

GI	*Genomic location*	*Start*	*End*	*Size (bp)*	*GC content (%)*	*No. of genes*	*No. of hypothetical proteins*	*Inferred function*[a]	*Codon usage deviation*[b]
1	Chromosome	96 164	120 611	24 447	0.61	23	6	Transposase	3.44
2	Chromosome	153 291	175 977	22686	0.64	18	8	Mixed	2.02
3	Chromosome	404 107	424 984	20877	0.64	20	5	Restriction enzyme	1.52
4	Chromosome	429 137	454 285	25148	0.66	23	5	Lipid metabolism	1.54
5	Chromosome	552 943	578 723	25780	0.67	20	19	Hypothetical/phage	1.38
6	Chromosome	957 476	984 789	27 313	0.59	23	7	Amino-acid metabolism	2.90
7	Chromosome	985 606	1023 177	37571	0.62	28	11	Phage	1.19
8	Chromosome	1041 719	1062 926	21207	0.62	22	10	Phage	2.19
9	Chromosome	1357 276	1382 924	25648	0.67	25	12	Urease	2.00
10	Chromosome	1510 936	1541 310	30374	0.64	24	12	Mixed	2.02
11	Chromosome	1629 336	1650 536	21200	0.63	24	5	Transposase	2.14
12	Chromosome	1992 883	201 4418	21535	0.63	24	17	Phage	1.81
13	Chromosome	2108 360	2132 880	24520	0.62	19	10	Transposase	1.70
14	Chromosome	2417 132	2437 558	20426	0.66	11	2	Integrase	3.61
15	Chromosome	2470 089	2497 491	27402	0.64	23	12	CRISPR	2.47
16	Chromosome	2767 330	2788 299	20969	0.65	13	5	Phage	1.50
17	Chromosome	2789 488	2812 846	23358	0.62	21	10	Mixed	3.58
18	Chromosome	2979 228	299 9796	20568	0.64	20	12	Mixed	1.66
19	Chromosome	3086 134	310 7437	21303	0.62	17	9	Lipid	1.68
20	Chromosome	311 1453	313 9687	28234	0.66	9	3	Restriction enzyme	2.08
21	Chromosome	3718 652	3745 552	26900	0.59	18	10	Mixed	4.57
22	Chromosome	3863 660	3888 823	25163	0.61	18	7	Cell regulation	3.83
23	Chromosome	4038 451	4058 699	20248	0.58	19	17	Hypothetical	4.16
24	Chromosome	4165 663	4195 266	29603	0.68	17	13	Hypothetical	2.12
25	Chromosome	4541 945	4564 362	22417	0.66	21	9	Membrane transport	1.57
26	Chromosome	4803 748	483 6560	32812	0.66	11	2	Mixed	3.06
27	Chromosome	498 6842	5013 397	26555	0.60	27	10	Transposase	1.68
28	168-kbp Plasmid	8114	49876	41762	0.61	37	22	Phage/tranposase	2.18

Abbreviations: CRISPR, Clustered Regularly Interspaced Short Palindromic Repeats; GC, guanine–cytosine; GI, gastrointestinal.
[a]Mixed, multiple genes present in the GI with varied functions.
[b]Sum of the differences in codon use for each triplet between an island and the genome.

IA or transferred into Clade IIA UW-1 long enough to allow for codon usage to converge. In addition, some of these GIs may have been a result of predation and integration into the Clade IIA genome just before collecting the sample R104-IIA. We note that it is possible that some of the identified GIs were missing in the Clade IA scaffolds because of the removal of reads sharing high identity with Clade IIA UW-1 during the preassembly screening for sample R107-IA, although the presence of genes involved in horizontal transfer provides support for the likelihood that they are indeed GIs.

Similarly, we searched for GIs in the Clade IA scaffolds by recruiting genes from the finished Clade IIA UW-1 genome. We identified five Clade IA GIs that contained 129 genes (Table 4). Of these, 93 genes (72%) were annotated as hypothetical genes. Interestingly, GI 4, which appears to be derived from foreign DNA based on having the largest codon usage deviation, is entirely comprised of hypothetical genes. When these genes were compared using blast against the NCBI non-redundant database (nr), no significant blast hits (e-value <1) were obtained for any of these genes. The largest GI in Clade IA was over 50 kbp long and contained a mix of hypothetical and phage-related genes. Despite the large fraction of phage genes, this GI had the smallest codon usage deviation, implying that the island was due to lysogenic phage integration less recently than in other islands. GI 1 contained genes for several membrane proteins. With the codon usage similar to the average value, it is likely that this is simply a region of unique gene functions and not recently horizontally transferred. Similar to GI 4, very few of these genes had significant blast hits with sequences in the nr database. Surprisingly, Scaffold00028, which is entirely a GI 2, is nearly identical ($>98\%$ similar over 92% of its length) to a podovirus (EPV 1) sequenced in a viral metagenome (Skennerton *et al.*, 2011) generated from the same bioreactor 7 months after the R104-IIA sample and roughly 2.5 years earlier when the R107-IA sample was collected. Based on having similar coverage and tetranucleotide frequencies to Clade IA scaffolds, we believe that this is a lysogenic phage in the Clade IA genome. The only differences between the EPV 1 scaffold and GI 2 are two non-contiguous $\sim$1000-bp regions that contain hypothetical genes.

Genetic basis for ecophysiological differentiation

Previous studies using Accumulibacter-enriched bioreactors have suggested that Clade IA can reduce nitrate, whereas Clade IIA cannot (Carvalho *et al.*, 2007; Flowers *et al.*, 2009; Guisasola *et al.*, 2009; Oehmen *et al.*, 2010b). Clade IIA UW-1's inability to

Table 4 Characteristics of Clade IA UW-2 GIs

GI	Genomic location	Start	End	Size (bp)	GC content (%)	No. of genes	No. of hypothetical proteins	Inferred function[a]	Scaffold length (bp)	Codon usage deviation[b]
1	Scaffold00018	536 000	558 598	22 599	67	10	3	Mixed	814 144	2.63
2	Scaffold00028	0	35 006	35 007	59	48	39	Lysogenic phage	35 006	4.514
3	Scaffold00116	0	23 750	23 751	64	6	4	Hypothetical	425 836	2.73
4	Scaffold00116	24 856	45 841	20 985	68	10	10	Hypothetical	425 836	5.431
5	Scaffold01460	136 370	187 027	50 657	62	55	37	Phage	281 699	1.648

Abbreviations: GC, guanine–cytosine; GI, gastrointestinal.
[a]Mixed, multiple genes present in the GI with varied functions.
[b]Sum of the differences in codon use for each triplet between an island and the scaffolds.

reduce nitrate was also suggested as its genome lacked all of the subunits for the respiratory nitrate reductase gene (*narGHI*). Interestingly, no *nar* genes could be identified in the Clade IA scaffolds presented here. The Clade IIA UW-1 genome did contain identifiable periplasmic nitrate reductase (*napDAGHBF*) in a single gene cluster. There was also a *napC/nirT* homolog that has been shown in other organisms to be used with *nap* genes in another locus to perform nitrate reduction while providing enough proton-motive force for energy production (Gonzalez *et al.*, 2006). These same genes with nearly the same organization were also found in the Clade IA genome (Scaffold01135), except that the *napF* gene was missing; however, based on conserved operon structure in model organisms, the *napF* gene should have been located where a gap exists in the Clade IA scaffold. It is still possible that the gap exists as a result of the preassembly screening, which removed the *napF* gene because of having sequence homology $>97\%$, but this is unlikely given that the ANI of shared genes in this gene neighborhood was 83% (across 28 kbp). If Clade IA does use these *nap* genes for nitrate respiration, the observed differences in nitrate-reducing capabilities between these two clades might be related to gene regulation rather than gene content.

The metagenome assembly from sample R107-IA did contain a cluster of *narGHIJ* genes on Scaffold00577, which is $\sim$13 kbp long (6 kbp when excluding Ns), but the mean coverage for this scaffold ($5\times$) is very low as compared with the Clade IA scaffolds (16.2 X). The best hits to the scaffold obtained using NCBI's blastx against nr were to the genera *Intrasposrangium*, *Serinicoccus* and *Janibacter* (members of the *Actinobacteria* phylum), suggesting a different origin. Still, given the fact that the Accumulibacter Clade IA genome is not complete, the absence of *narGHIJ* genes within the Accumulibacter Clade IA genome cannot be confirmed currently.

Clade IIA UW-1 had genes required for nitrogen fixation and carbon fixation, but most of these genes appear to be absent in the Clade IA genome because they were not found in the Clade IA scaffolds or at significantly high read coverage in the metagenome. Specifically, Clade IA lacked two of the important genes required for the Calvin cycle, ribulose-1, 5-bisphosphate carboxylase oxygenase (*rubisco*) and ribulose-phosphate 3-epimerase (*Rpe*), which were present in Clade IIA UW-1 (JGI-IMG/M gene OID: 2 014 613 882 and 2 014 614 231, respectively). Also, Clade IA contained none of the nitrogenase subunits, *nifDHK*, present in the Clade IIA UW-1 genome. The absences of these genes might be explained by a loss over time because of being present in our bioreactors for multiple years or may indicate that Clade IA originated from natural environments where nitrogen and carbon fixation are not required. Of course, it is also possible that the draft Clade IA genome lacked these genes because of incomplete genome coverage or assembly. To assess this likelihood, we searched for these genes in other scaffolds and among the raw metagenomic reads. However, we found no definitive evidence for the presence of these genes in the Clade IA genome (see Supplementary Online Material). Additional sequencing and further assembly will need to be done to confirm these gene-level differences between Clade IA and IIA.

Comparison of CRISPR loci

CRISPR elements are thought to provide resistance to invasion of phage or other foreign DNA by storing segments of previously confronted phage or other foreign DNA as spacers that are surrounded by short palindromic-like repeat sequences adjacent to a series of CRISPR-associated genes (CAS) (Barrangou *et al.*, 2007; Marraffini and Sontheimer, 2010). The detection of CRISPRs in a genome is significant because the presence or absence of these loci can determine which populations remain after a viral predation event. In a previous study, Accumulibacter Clade IIA UW-1 was thought to contain three CRISPR loci, whereas the genome was still in a draft form (Kunin *et al.*, 2008); however, the finished genome contained only two. Here, we found that the Clade IA scaffolds only contained one CRISPR locus

Table 5 Summation of CRISPR loci in Accumulibacter Clades IA and IIA

Loci	*Clade*	*Location*	*Start*	*End*	*CAS gene structure*	*No. of spacers*	*No. of virome match*[a]
CR1	IIA	Chromosome	2 475 140	2 479 958	cas2-cas1-cas2-TM812-Cmr(6–2)	64	0
CR2	IIA	Chromosome	2 565 609	2 575 272	cas3-cse1-cse2-cse4-cas5-cse3-cas1-cas2	155	0
CR3	IA	Scaffold00018	141 165	147 645	cas3-cse1-cse2-cse4-cas5-cse3-cas1-cas2	100	9

Abbreviation: CRISPR, Clustered Regularly Interspaced Short Palindromic Repeats.
[a]The value counts the number of spacer sequences that had complete matches based on blast alignment to the virome sample collected from the bioreactor 7 months after the R104-IIA sample (Skennerton *et al.*, 2011).

(Table 5). Interestingly, the CRISPR repeat sequences and CAS gene structure in the two Clade IIA UW-1 loci were different. The CRISPR locus in Clade IA did not share any repeat sequences with the loci in Clade IIA UW-1; however, the CAS gene order and predicted function in Clade IA (CR3) were identical to those present in one of the Clade IIA UW-1 loci (CR2). Despite the similar gene order and predicted function, the genes appear to have different origins based on low sequence similarities. Comparison of the spacers in the three loci using blastn determined that there were no spacers shared among them. Interestingly, blast analysis of the spacer sequences from all three loci with the viral metagenome (Skennerton *et al.*, 2011), generated from the same bioreactor 7 months after the R104-IIA sample and roughly 2.5 years before the R107-IA sample, yielded only perfect matches with the Clade IA CRISPR Spacers (Table 5). In total, nine Clade IA CRISPR spacers matched perfectly with the EPV1 phage that was found to be a likely lysogen in the Clade IA genome (Scaffold00028 corresponding to GI 2). In contrast, neither of the Clade IIA CRISPR regions matched any viral metagenomic sequences completely. Skennerton *et al.* (2011) predicted that this phage was specific for Accumulibacter and they also noted the presence of a histone-like nucleoid-structuring (H-NS) protein that might make the phage resistant to CRISPR activity. The repeated presence of phage DNA in CRISPR spacers, particularly near the leader region (which represent the most current phage insertion events), suggest that the histone-like nucleoid structuring allows for EPV1 to infect continually Clade IA. This suggests that these same phage populations or similar types were still active 2.5 years later during the time of collecting the R107-IA sample, and that only Clade IA is susceptible to predation by the EPV1 phage in this system.

Metabolic reconstruction of Accumulibacter Clade IA

Some elements of EBPR metabolism have been under contention for several decades now. The main area of disagreement is the source and balancing of anaerobic-reducing equivalents for polyhydroxyalkanoate production. Researchers disagree about the pathway used for anaerobic operation of glycolysis (Embden–Meyerhof–Parnas versus Entner–Douderoff (ED) pathway) and the direction of the TCA cycle (reductive, split, full or through glyoxylate shunt) (Oehmen *et al.*, 2007). The finished genome of Accumulibacter Clade IIA UW-1 revealed that it only contained genes for the Embden–Meyerhof–Parnas pathway and also showed the presence of all genes necessary for the varied modes of the TCA cycle previously suggested for EBPR (Garcia Martin *et al.*, 2006). Not too surprisingly, the draft Clade IA genome also contained nearly all of the important genes associated with EBPR metabolism, and also lacked ED pathway genes. The only important EBPR-related gene that seemed to be absent in the Clade IA genome encodes the E1 subunit of the pyruvate dehydrogenase complex; however, the other subunits for the pyruvate dehydrogenase complex were present and there is a gap in the scaffold where the E1 subunit should be located. Therefore, it is likely that this missing gene will be found in the finished genome. Although the overall gene content was nearly identical, there were differences in gene counts between the two organisms. For example, Clade IA contained two copies of the fumarase (fig|759355.3.peg.2281 and fig|759355.3.peg.1714), whereas Clade IIA only contains one (JGI-IMG/M gene OID: 645 011 516). Whether the additional fumarase in Clade IA is expressed anaerobically needs to be determined by future gene expression analysis. One interesting discovery was the existence of three Na(+)-translocating NADH-quinone reductase (Rnf/Nqr) encoding gene clusters in Clade IIA (IMG/M gene OID: 645 012 180–645 012 185 and 645 010 733–645 010 738 and 645 012 144–645 012 149) as compared with a single such cluster in the Clade IA genome (fig|759355.3.peg.2984–2978). One of the Clade IIA clusters (IMG/M gene OID: 645 010 733–645 010 738) was relatively homologous (>81% amino acid similarity) with Clade IA, but the remaining two Clade IIA operons (IMG/M gene OID: 645 012 144–645 012 149 and 645 012 180–645 012 185) were much more divergent (<68% similar) from the Clade IA operon. Also, one of those operons had only three of the six subunits with any nucleotide similarity (<63%) to *Clade IA* genes. Although the function of these unique gene clusters in Clade IIA is unknown, it as well as the

other clusters share nearly identical structure (i.e. gene order) with *rnf* gene clusters that have been shown to catalyze the transfer or electron from reduced ferredoxin to NAD^+ coupled with Na^+ translocation (Muller *et al.*, 2008). If either of these gene clusters are expressed anaerobically, the Rnf/Nqr might assist in anaerobic operation of the TCA cycle since any reduced ferredoxin from pyruvate ferredoxin:oxidoreductase or α-ketoglutarate oxidoreductase can be used to produce NADH as well as a proton motive force for ATP production anaerobically.

In the original report of the Accumulibacter Clade IIA UW-1-enriched metagenome, several interesting findings were discussed including the presence of a novel fusion protein consisting of a cytochrome *b/b6* domain with several transmembrane helices as well as a NAD(P)- and flavin-binding domain. The fusion protein is proposed to allow for oxidation of reduced quinone from succinate dehydrogenase in the absence of oxygen by transferring electrons to NAD^+ and FAD (Garcia Martin *et al.*, 2006). Since then, the genomes of two strains of *Alicycliphilus denitrificans* (BC and K601), which were isolated from a wastewater treatment plant, were found to have an protein with homologous structure (Mechichi *et al.*, 2003; Weelink *et al.*, 2008; Oosterkamp *et al.*, 2011). We determined that the wrong gene id (JGI-IMG/M gene OID: 2 001 028 710 or 645 009 129 in finished genome) was provided for the novel cytochrome in that report rather than the actual protein with these domains (JGI-IMG/M gene OID: 2 001 028 680 or 645 009 126 on finished genome), so recent studies exploring its expression targeted the wrong gene (Burow *et al.*, 2008; He *et al.*, 2010b). Thus, its role in anaerobic metabolism is still unproven. We discovered that these two genes (JGI-IMG/M gene OID: 645 009 129 and 645 009 126) have orthologs in Clade IA (fig|759355.3.peg.563 and fig|759355.3.peg.561) with 81% and 86% nucleotide identity, respectively, that appear to be part of a conserved operon (Supplementary Figure S3). In addition, Clade IA region shares a larger nine-gene cluster (fig|759355.3.peg.561–fig|759355.3.peg.570) in that region with both strains of *Alicycliphilus denitrificans*. The additional sequences are all related to cytochrome *c* biosynthesis (Supplementary Figure S3). Despite having similar synteny to *Alicycliphilus*, the Clade IA novel fusion proteins are more similar to Clade IIA than to their homologs in *Alicycliphilus*, suggesting that Clades IA and IIA are more likely to have a common origin despite having different operon structure. What impact these different operon structures have on metabolism is yet to be determined.

Conservation of EBPR genes

We postulated that genes associated with the hallmark carbon and phosphorus cycling pathways in EBPR metabolism were under significant selective pressure because of their importance to the fitness of the bacteria in the EBPR ecosystems. To test this, we evaluated the level of conservation of EBPR genes as compared with genes not associated with EBPR (NON-EBPR genes) (Supplementary Table S3). Using the Student's *t*-test, we determined that the average nucleotide identities between these two clades for the EBPR and NON-EBPR genes, 82% and 78%,respectively, were statistically different ($P<0.00001$). In contrast to observed structural and gene content differences between the clades, the higher level of conservation for EBPR genes probably suggests that these important genes are under the same selective pressure. This idea is further supported by EBPR genes having a synonymous and non-synonymous substitution ratio of 0.05 that is also significantly different ($P<0.005$) than the synonymous and non-synonymous substitution ratio for NON-EBPR genes (0.07). These results suggest that mutations in EBPR genes are under stronger negative selection since mutations that cause amino-acid sequences changes are selected against more than in NON-EBPR genes.

Discussion

Before this work, several lines of evidence pointed to the existence of multiple distinct Accumulibacter clades in EBPR systems, despite the high 16S rRNA sequence identity within the Accumulibacter lineage (McMahon *et al.*, 2010). Although the R104-IIA sludge sample was enriched in Clade IIA, reads from closely related co-occurring species and strains were detected in its metagenome (Garcia Martin *et al.*, 2006). At that time, Accumulibacter lineage diversity was poorly characterized. Subsequently, a rigorous phylogenetic analysis based on the *ppk*1 locus was used to partition the lineage into two Types (I and II), which could be further subdivided into five and seven clades, respectively (He *et al.*, 2007; Peterson *et al.*, 2008).

In this study, we compared the gene content between representatives of Accumulibacter Clades IA and IIA. Although the complete genome for Clade IIA UW-1 is available, the genome for Clade IA was constructed by first removing reads, which were highly similar to Clade IIA UW-1 ($\geqslant$ 97%) from the metagenomic sequencing reads of sample R107-IA and assembling the remaining reads. The removal of these reads helped in preventing the development of a mosaic genome comprised of both Clade IA- and IIA-derived reads, but it also likely caused gaps in the Clade IA scaffolds in regions where there was high sequence conservation between Clades IA and IIA. From all of the assembled scaffolds, the Clade IA fragments were identified based on having tetranucleotide frequencies similar to Clade IIA UW-1. The limitation of this method to identify accurately fragments below 20 kbp likely reduced the number of Clade IA fragments that could be

identified. As a result, the assembly of this genome is considered as a draft and comparisons between Clade IA and IIA populations are considered preliminary. Despite these limitations, this novel approach allowed for assembly of large genomic fragments of our target organism from a mixed community that contained an organism of similar phylogeny and function. The assembly was considered effective as indicated by the high level of estimated completeness (80–90%) of the genome based on the presence of essential COG functions, and specifically tRNAs, tRNA synthetases and ribosomal proteins.

Comparison of genes related to EBPR metabolism (including those involved in central carbon metabolism) did not reveal any marked differences between the two clades. Previous studies suggested that these two clades used the glycolytic and TCA cycle differently under anaerobic conditions (Wexler *et al.*, 2009; Oehmen *et al.*, 2010a; Acevedo *et al.*, 2012). Although we did not detect any apparent genome-level differences, we did note instances where the gene copy number for a particular enzyme important in the TCA cycle varied, which could influence expression levels. Specifically, we noticed a higher abundance of a protein complex (Na(+)-translocating NADH-quinone reductase) in Clade IIA, which may allow for it to operate either a reductive or complete TCA cycle anaerobically. Although Clade IA did contain a single gene cluster encoding this complex, it is possible that these genes are not expressed or have another function for Clade IA that is yet to be determined.

With highly conserved 16S rRNA sequences (98.5%) and similar functions in EBPR processes, the genomes of these two clades were expected to have similar genomic structure and gene content originating from a common ancestor. However, our results suggest that these two clades are significantly different in both characteristics. Accumulibacter Clades IA and IIA only have 25% of their genomes exhibiting any synteny and they only share an estimated 63% and 48% of their gene content, respectively, at an ANI of 78%. The sequencing of a sludge sample enriched in Clade IA has revealed significant genome-level differentiation between the two clades, which could arguably be considered as two 'species' of Accumulibacter.

Several GIs were identified in both clades. We identified 28 putative GIs in Clade IIA UW-1 that contained a variety of genes including phage-related genes. Contrastingly, Clade IA only had five putative GIs in its scaffolds with inferred characteristics ranging from phage-related to hypothetical. When considering the functions of the genes and the codon usage deviations in the GIs, it is likely that many of these differences are associated with foreign DNA integration into each genome. Because the Clade IA genome is not complete, several of the putative GIs in Clade IIA UW-1 are probably associated with regions currently missing in the Clade IA scaffolds; however, it was surprising that only five GIs existed in Clade IA totaling 150 kbp (~3% of the scaffold length) considering the fact that such a large fraction of the total genes lacked orthologs in Clade IIA UW-1. This indicates that while there are large genomic differences, the location of these differences are sprinkled throughout the genome and not restricted to specific regions. This idea is supported by viewing the genome alignments, which revealed a spider web of matching regions between the genomes (Supplementary Figure S1).

The genes associated with EBPR metabolism appear to be the exception to the general interspecies differences, as they all are present in both clades and share an ANI of 81%, which is higher than the average for the two genomes. It is possible that these genes, which are thought to be essential for EBPR performance, are diverging less. This idea is supported by the EBPR genes having an average synonymous and non-synonymous substitution ratio of 0.05, which is statistically lower than that of the NON-EBPR genes (0.07).

A previous long-term studies on our bioreactors have shown extended periods of both Clade IA and Clade IIA dominance (He *et al.*, 2010a). It is possible that changes in the community structure were associated with phage predation events that specifically targeted each clade. In theory, the additional CRISPR locus in the Clade IIA genome should provide it with more resistance to phage predation because of the presence of more phage spacer sequences (221 versus 100) and lessen the likelihood of phage predation, but recent papers have shed light on possible mechanisms by which phages counteract the CRISPR activity including a podovirus identified in the viral metagenome from our bioreactors(Skennerton *et al.*, 2011; Bondy-Denomy *et al.*, 2013). The persistence of viral populations despite CRISPR spacer matches present in the bacterial genomes is supported by the detection of spacers located near the leader region, which have high identity to a partially assembled phage from a viral metagenome (Skennerton *et al.*, 2011) sampled 2.5 years earlier as well as the apparent presence of the same lysogenic phage in the Clade IA genome.

One of the more interesting findings in this study was the apparent conservation of some pieces of the Accumulibacter Clade IIA UW-1 genome and loss of others. Specifically, there is evidence that either the plasmids or plasmid-associated genes are retained within the Clade IA genome. It is currently unclear if these scaffolds are derived from a new plasmid or from chromosomal fragments, but the large number of genes associated with conjugation suggested plasmid origin. The plasmids from Accumulibacter Clade IIA UW-1 mostly contained genes associated with conjugation, transposases and heavy metal resistance, but one of the Clade IA scaffolds that may be plasmid derived (Scaffold01134) contains numerous genes associated with important functions

including cytochromes, ubiquinol-cytochrome *C* reductase and PHA synthase. One surprising finding during the sequencing of Clade IIA UW-1 was the presence of carbon and nitrogen fixation genes, considering the fact that wastewater is a carbon- and nitrogen-rich environment. The Clade IA scaffolds lack most of the genes associated with these processes; however, there is some weak evidence that these genes were simply removed during the preassembly screen of the R107-IA raw reads. Whether this gene loss reflects the genomic structure of 'wild' Clade IA populations, is a result of natural gene loss over time spent in the bioreactor or an artifact due to removal of reads during the preassembly screen remains to be determined.

Conclusion

Through metagenomic sequencing of a Clade IA-enriched lab-scale bioreactor, a large fraction of the genome for Clade IA was assembled. Some of the results from this study are still preliminary because of the required treatment to Clade IIA UW-1-like sequence reads to avoid a mosaic Clade IA and IIA genome. Nevertheless, the study does reveal that while Clades IA and IIA have all of the necessary genes for EBPR metabolism and nitrite reduction, there are marked genomic differences between the two clades. Specifically, there is little genome synteny between the two clades and there appears to be differences in their ability to fix carbon and nitrogen. In addition, Accumulibacter Clade IIA UW-1 may have better defenses against phage predation based on the presence of an additional CRISPR locus as compared with Clade IA. Overall, these findings provide a greater understanding of the differences between these two clades and will assist in further exploration of metabolic differences through future gene expression studies.

Conflict of Interest

The authors declare no conflict of interest.

Acknowledgements

We thank Francisco Rodriguez-Valera, Rohit Ghai and Ana Belén Martín Cuadrado at the Universidad Miguel Hernandez in Alicante, Spain, for insightful discussion, ideas for analysis and access to custom perl scripts, and Forest Bishop, Alisha Truman and Nick Bartolerio for assistance with running bioreactors. We also thank Ben Oyserman for thoughtful comments on early drafts of the manuscript. KDM acknowledges funding from the US National Science Foundation (CBET-0967646) and the UW-Madison Graduate School. The work conducted by the US Department of Energy Joint Genome Institute is supported by the Office of Science of the US Department of Energy under Contract No. DE-AC02–05CH11231.

References

Abe T, Kanaya S, Kinouchi M, Ichiba Y, Kozuki T, Ikemura T. (2003). Informatics for unveiling hidden genome signatures. *Genome Res* **13**: 693–702.

Acevedo B, Oehmen A, Carvalho G, Seco A, Borras L, Barat R. (2012). Metabolic shift of polyphosphate-accumulating organisms with different levels of polyphosphate storage. *Water Res* **46**: 1889–1900.

Altschul SF, Madden TL, Schaffer AA, Zhang J, Zhang Z, Miller W *et al.* (1997). Gapped BLAST and PSI-BLAST: a new generation of protein database search programs. *Nucleic Acids Res* **25**: 3389–3402.

Aziz RK, Bartels D, Best AA, DeJongh M, Disz T, Edwards RA *et al.* (2008). The RAST server: rapid annotations using subsystems technology. *BMC Genom* **9**: 75.

Barrangou R, Fremaux C, Deveau H, Richards M, Boyaval P, Moineau S *et al.* (2007). CRISPR provides acquired resistance against viruses in prokaryotes. *Science* **315**: 1709–1712.

Bondy-Denomy J, Pawluk A, Maxwell KL, Davidson AR. (2013). Bacteriophage genes that inactivate the CRISPR/Cas bacterial immune system. *Nature* **493**: 429–432.

Burow LC, Mabbett AN, Blackall LL. (2008). Anaerobic glyoxylate cycle activity during simultaneous utilization of glycogen and acetate in uncultured Accumulibacter enriched in enhanced biological phosphorus removal communities. *ISME J* **2**: 1040–1051.

Carvalho G, Lemos PC, Oehmen A, Reis MAM. (2007). Denitrifying phosphorus removal: linking the process performance with the microbial community structure. *Water Res* **41**: 4383–4396.

Carver TJ, Rutherford KM, Berriman M, Rajandream M-A, Barrell BG, Parkhill J. (2005). ACT: the Artemis comparison tool. *Bioinformatics* **21**: 3422–3423.

Chou H-H, Holmes MH. (2001). DNA sequence quality trimming and vector removal. *Bioinformatics* **17**: 1093–1104.

Crocetti GR, Hugenholtz P, Bond PL, Schuler A, Keller J, Jenkins D *et al.* (2000). Identification of polyphosphate accumulating organisms and the design of 16S rRNA-directed probes for their detection and quantitation. *Appl Environ Microbiol* **66**: 1175–1182.

Darling AE, Mau B, Perna NT. (2010). ProgressiveMauve: multiple genome alignment with gene gain, loss and rearrangement. *PLoS One* **5**: e11147.

Edgar RC. (2004). MUSCLE: multiple sequence alignment with high accuracy and high throughput. *Nucleic Acids Res* **32**: 1792–1797.

Flowers JJ, He S, Yilmaz S, Noguera DR, McMahon KD. (2009). Denitrification capabilities of two biological phosphorus removal sludges dominated by different '*Candidatus Accumulibacter*' clades. *Environ Microbiol Rep* **1**: 583–588.

Garcia Martin H, Ivanova N, Kunin V, Warnecke F, Barry KW, McHardy AC *et al.* (2006). Metagenomic analysis of two enhanced biological phosphorus removal (EBPR) sludge communities. *Nat Biotechnol* **24**: 1263–1269.

Gilbert JA, Dupont CL. (2011). Microbial metagenomics: beyond the genome. In: Carlson CA, Giovannoni SJ (eds) *Annual Review of Marine Science* Vol. 3. Annual Reviews: Palo Alto, pp 347–371.

Gonzalez PJ, Correia C, Moura I, Brondino CD, Moura JJG. (2006). Bacterial nitrate reductases: molecular and

biological aspects of nitrate reduction. *J Inorg Biochem* **100**: 1015–1023.

Guisasola A, Qurie M, MdM Vargas, Casas C, Baeza JA. (2009). Failure of an enriched nitrite-DPAO population to use nitrate as an electron acceptor. *Process Biochem* **44**: 689–695.

He S, Bishop FI, McMahon KD. (2010a). Bacterial community and Accumulibacter population dynamics in biological phosphorus removal sludge. *Appl Environ Microbiol* **76**: 5479–5487.

He S, Gall DL, McMahon KD. (2007). '*Candidatus Accumulibacter*' population structure in enhanced biological phosphorus removal sludges as revealed by polyphosphate kinase genes. *Appl Environ Microbiol* **73**: 5865–5874.

He S, Gu AZ, McMahon KD. (2008). Progress towards understanding the distribution of Accumulibacter among full-scale enhanced biological phosphorus removal systems. *Microb Ecol* **55**: 229–236.

He S, Kunin V, Haynes M, Garcia Martin H, Ivanova N, Kyrpides N *et al.* (2010b). Metatranscriptomic analysis of 'Candidatus Accumulibacter'-enriched enhanced biological phosphorus removal sludge. *Environ Microbiol* **12**: 1205–1217.

He S, McMahon KD. (2011). 'Candidatus Accumulibacter' gene expression in response to dynamic EBPR conditions. *ISME J* **5**: 329–340.

Hesselmann RPX, Werlen C, Hahn D, van der Meer JR, Zehnder AJB. (1999). Enrichment, phylogenetic analysis and detection of a bacterium that performs enhanced biological phosphate removal in activated sludge. *System Appl Microbiol* **22**: 454–465.

Kettler GC, Martiny AC, Huang K, Zucker J, Coleman ML, Rodrigue S *et al.* (2007). Patterns and implications of gene gain and loss in the evolution of Prochlorococcus. *PLoS Genet* **3**: 2515–2528.

Kunin V, He S, Warnecke F, Peterson SB, Martin HG, Haynes M *et al.* (2008). A bacterial metapopulation adapts locally to phage predation despite global dispersal. *Genome Res* **18**: 293–297.

Li W, Godzik A. (2006). Cd-hit: a fast program for clustering and comparing large sets of protein or nucleotide sequences. *Bioinformatics* **22**: 1658–1659.

Marraffini LA, Sontheimer EJ. (2010). CRISPR interference: RNA-directed adaptive immunity in bacteria and archaea. *Nat Rev Genet* **11**: 181–190.

McMahon KD, Dojka MA, Pace NR, Jenkins D, Keasling JD. (2002). Polyphosphate kinase from activated sludge performing enhanced biological phosphorus removal. *Appl Environ Microbiol* **68**: 4971–4978.

McMahon KD, He S, Oehmen A. (2010). *The microbiology of phoshorus removal* In: Seviour RJ, Nielsen PH (eds)Microbial Ecology of Activated SludgeIWA Publishing: London, pp 281–320.

Mechichi T, Stackebrandt E, Fuchs G. (2003). *Alicycliphilus denitrificans* gen. nov., sp. nov., a cyclohexanol-degrading, nitrate-reducing Œ≤-proteobacterium. *Int J Syst Evol Microbiol* **53**: 147–152.

Mino T, Van Loosdrecht MCM, Heijnen JJ. (1998). Microbiology and biochemistry of the enhanced biological phosphate removal process. *Water Res* **32**: 3193–3207.

Muller V, Imkamp F, Biegel E, Schmidt S, Dilling S. (2008). Discovery of a ferredoxin: NAD(+)-oxidoreductase (Rnf) in acetobacterium woodii—a novel potential coupling site in acetogens. In: Wiegel J, Maier RJ, Adams MWW (eds) *Incredible Anaerobes: From Physiology to Genomics to Fuels*. Blackwell Publishing: Oxford, pp 137–146.

Oehmen A, Carvalho G, Freitas F, Reis MAM. (2010a). Assessing the abundance and activity of denitrifying polyphosphate accumulating organisms through molecular and chemical techniques. *Water Sci Technol* **61**: 2061–2068.

Oehmen A, Carvalho G, Freitas F, Reis MAM. (2010b). Assessing the abundance and activity of denitrifying polyphosphate accumulating organisms through molecular and chemical techniques. *Water Sci Technol* **61**: 2061–2068.

Oehmen A, Carvalho G, Lopez-Vazquez CM, van Loosdrecht MCM, Reis MAM. (2010c). Incorporating microbial ecology into the metabolic modelling of polyphosphate accumulating organisms and glycogen accumulating organisms. *Water Res* **44**: 4992–5004.

Oehmen A, Lemos PC, Carvalho G, Yuan Z, Keller J, Blackall LL *et al.* (2007). Advances in enhanced biological phosphorus removal: from micro to macro scale. *Water Res* **41**: 2271–2300.

Oosterkamp MJ, Veuskens T, Plugge CM, Langenhoff AAM, Gerritse J, van Berkel WJH *et al.* (2011). Genome sequences of *Alicycliphilus denitrificans* strains BC and K601T. *J Bacteriol* **193**: 5028–5029.

Penn K, Jensen PR. (2012). Comparative genomics reveals evidence of marine adaptation in *Salinispora* species. *BMC Genom* **13**: 86.

Peterson SB, Warnecke F, Madejska J, McMahon KD, Hugenholtz P. (2008). Environmental distribution and population biology of the genus Accumulibacter, a primary agent of biological phosphorus removal in activated sludge. *Environ Microbiol* **10**: 2692–2703.

R Development Core Team (2009). *R: A Language and Environment for Statistical Computing*. R Foundation for Statistical Computing*Vienna, Austria.*

Reno ML, Held NL, Fields CJ, Burke PV, Whitaker RJ. (2009). Biogeography of the *Sulfolobus islandicus* pan-genome. *Proc Natl Acad Sci* **106**: 8605–8610.

Rice P, Longden I, Bleasby A. (2000). EMBOSS: The European Molecular Biology Open Software Suite. *Trends Genet* **16**: 276–277.

Rusch DB, Halpern AL, Sutton G, Heidelberg KB, Williamson S, Yooseph S *et al.* (2007). The Sorcerer II Global Ocean Sampling expedition: Northwest Atlantic through Eastern Tropical Pacific. *PLoS Biol* **5**: 398–431.

Skennerton C, Angly F, Breitbart M, Bragg J, He S, Hugenholtz P *et al.* (2011). Phage encoded H-NS: a potential Achilles heel in the bacterial defence system. *PLoS One* **6**: e20095.

Suyama M, Torrents D, Bork P. (2006). PAL2NAL: robust conversion of protein sequence alignments into the corresponding codon alignments. *Nucleic Acids Res* **34**: W609–W612.

Teeling H, Meyerdierks A, Bauer M, Amann R, Glockner FO. (2004). Application of tetranucleotide frequencies for the assignment of genomic fragments. *Environ Microbiol* **6**: 938–947.

Weelink SAB, Tan NCG, ten Broeke H, van den Kieboom C, van Doesburg W, Langenhoff AAM *et al.* (2008). Isolation and characterization of *Alicycliphilus denitrificans* strain BC, which grows on benzene with chlorate as the electron acceptor. *Appl Environ Microbiol* **74**: 6672–6681.

Wexler M, Richardson DJ, Bond PL. (2009). Radiolabelled proteomics to determine differential functioning of Accumulibacter during the anaerobic and aerobic phases of a bioreactor operating for enhanced biological phosphorus removal. *Environ Microbiol* **11**: 3029–3044.

Wilmes P, Andersson AF, Lefsrud MG, Wexler M, Shah M, Zhang B *et al.* (2008). Community proteogenomics highlights microbial strain-variant protein expression within activated sludge performing enhanced biological phosphorus removal. *ISME J* **2**: 853–864.

Yang ZH. (2007). PAML 4: Phylogenetic analysis by maximum likelihood. *Mol Biol Evol* **24**: 1586–1591.

Zerbino DR, Birney E. (2008). Velvet: Algorithms for *de novo* short read assembly using de Bruijn graphs. *Genome Res* **18**: 821–829.

Supplementary Information accompanies this paper on The ISME Journal website (http://www.nature.com/ismej)